Vol 18 No 7, July 2009
1674-1056/2009/18(07)/2839-07

Chinese Physics B

© 2009 Chin. Phys. Soc.
and IOP Publishing Ltd

Temporal behaviour of open-circuit photovoltaic solitons*

Zhang Mei-Zhi(张美志)[a)b)†], Lu Ke-Qing(卢克清)[a)], Cheng Guang-Hua(程光华)[a)],
Li Ke-Hao(李可昊)[a)b)], Zhang Yi-Qi(张贻齐)[a)b)],
Zhang Yu-Hong(张玉虹)[a)b)], and Zhang Yan-Peng(张彦鹏)[c)]

[a)] *State Key Laboratory of Transient Optics and Photonics, Xi'an Institute of Optics and Precision Mechanics, Chinese Academy of Sciencess, Xi'an* 710119, *China*
[b)] *Graduate School of Chinese Academy of Sciences, Beijing* 100039, *China*
[c)] *Department of Electronic Science and Technology, Xi'an Jiaotong University, Xi'an* 710049, *China*

(Received 23 September 2008; revised manuscript received 8 March 2009)

Based on the time-dependent band-transport model in a photorefractive medium, dark open-circuit photovoltaic (PV) solitons are investigated both theoretically and experimentally. Compared with those of the time-independent models, our theoretical results revealed that quasi-steady-state and steady-state PV solitons can both be obtained. Our results also revealed that when $r < 1$ (r is the normalized intensity at infinity), the full width at half maximum (FWHM) of solitons decreases monotonically to a constant value; when $r > 1$, however, the FWHM of solitons first decreases to a minimum before it increases to a constant value. Moreover, the FWHM of steady solitons decreases with increasing intensity ratio for $r < 1$, and increases with increasing intensity ratio for $r > 1$. We further observed dark PV solitons in experiments, and recorded their evolution. These results indicated that steady solitons can be observed at low optical power, while quasi-steady-state solitons can only be generated at higher optical power. Good agreement is found between theory and experiment.

Keywords: temporal behaviour, photovoltaic solitons, photorefractive effect
PACC: 4265J, 4265S, 7240

1. Introduction

Over the past few years, photorefractive (PR) spatial solitons have attracted growing attention due to their potential applications in all-optical devices.[1] According to their different physical origins and characters, PR solitons can be classified into three types, i.e., quasi-steady-state solitons,[2,3] screening solitons[4] and photovoltaic(PV) solitons.[5,6] Quasi-steady-state solitons were first predicted in 1992,[2] and were observed in experiment in the next year. After that, bright and dark steady screening solitons were demonstrated with a background beam. The first theoretical model to explain quasi-steady-state solitons was based on the PR couple-mode theory.[2,7] Screening solitons were obtained by the solution of nonlinear Schrödinger equation in which the nonlinearity was given by a basic PR model.[8] This theory has been further developed to explain the beam self-deflection and solitons interaction.[9] The above theories show that the quasi-steady-state solitons and screening solitons have the same physical origin. PV solitons are different from other solitons because they do not need an external applied field but rely on the PV field. Dark PV solitons have been observed and induced slab waveguides[5,10] in $LiNbO_3$ crystal. Bright PV solitons have also been experimentally observed in sodium potassium strontium barium niobate (KNSBN).[11] From the pioneering work we find that the formation of PV solitons is similar to that of the screening solitons. We speculate that the PV solitons can be of quasi-steady-state and steady-state regimes. In light of quasi-steady-state solitons they have many merits, such as smaller external bias voltage, less formation time, independence of the beam intensity,[12] to deepen the study on them is meaningful work.

In this paper, based on the bias of the time-dependent band-transport model, we simulate the evolution of full width at half maximum (FWHM) of one-dimensional open-circuit dark PV solitons to show

*Project supported by the National Natural Science Foundation of China (Grant No 10674176).
†Corresponding author. E-mail: meizhi_zhang@126.com

that the quasi-steady-state and steady-state regimes can be treated together. The theory is confirmed by dark PV solitons experiments in $LiNbO_3$:Fe crystal. The experiments have revealed that PV solitons are observed in the steady-state regime at low beam power and in the quasi-steady-state regime at higher power. In our samples, steady-state solitons at high optical power were not achieved because of modulation instability.

2. Theory

To study the open-circuit dark PV solitons in PV material, we assume that a beam propagates along the z axis, which is allowed to diffract only along the x-direction $I_{\rm em}(x)$. Moreover, we assume that the beam is linearly polarized along the x coordinate. In the sole charge carrier time-dependent band-transport model, the standard set of rate and continuity equations and Gauss's law, which describe the PR effect[13−15] can be given by

$$\frac{\partial}{\partial t}N_{\rm d}^{+}=(\beta+sI_{\rm em})(N_{\rm d}-N_{\rm d}^{+})-\gamma nN_{\rm d}^{+}, \tag{1a}$$

$$\frac{\partial}{\partial x}(\varepsilon_0\varepsilon_{\rm r}E)=\rho, \tag{1b}$$

$$\frac{\partial J}{\partial x}+\frac{\partial \rho}{\partial t}=0, \tag{1c}$$

$$\rho=e(N_{\rm d}^{+}-N_{\rm a}-n), \tag{1d}$$

$$J=e\mu nE+\mu k_{\rm B}T\frac{\partial n}{\partial x}+\beta_{\rm ph}(N_{\rm d}-N_{\rm d}^{+})I_{\rm em}, \tag{1e}$$

where the five space- and time-dependent variables are the density of ionized donors $N_{\rm d}^{+}$, the electrons density n, the space-charge field inside crystal E, the charge density ρ, and the current density J. Relevant parameters of the crystal are: $N_{\rm d}$, the total donor density; $N_{\rm a}$, the density of ionized acceptors; β, the dark generation rate; s, the photoionization cross section; γ the recombination coefficient; μ the electron mobility; $\varepsilon_{\rm r}$, the relative dielectric constant at low frequency; and $\beta_{\rm ph}$, the photovoltaic constant. T is the temperature, ε_0 the vacuum permeability, $-e$ the electron charge, and $k_{\rm B}$ the Boltzmann's constant.

To obtain the relation between the space-charge field and the beam intensity, we make a hypothesis that the density of electrons in the crystal can be negligible compared with the density of ionized donors or acceptors, thus the density of ionized donors approximately equals that of the ionized acceptors ($N_{\rm d}^{+}\approx N_{\rm a}$). From Eqs.(1b) to (1e), one can deduce the relation of the space-charge field E, the beam intensity $I_{\rm em}$, and electron density n:

$$-\varepsilon_0\varepsilon_{\rm r}\frac{\partial^2 E}{\partial x\partial t}=e\mu\frac{\partial(nE)}{\partial x}+\mu k_{\rm B}T\frac{\partial^2 n}{\partial x^2}+\beta_{\rm ph}(N_{\rm d}-N_{\rm a})\frac{\partial I_{\rm em}}{\partial x}. \tag{2}$$

Assuming that steady state has been reached in Eq.(1), then the density of free electrons n can be expressed as

$$n=\frac{(\beta+sI_{\rm em})(N_{\rm d}-N_{\rm a})}{\gamma N_{\rm a}}. \tag{3}$$

By substituting Eq.(3) into Eq.(2), and integrating it with respect to x, one can obtain the differential equation of space-charge field and beam intensity as follows:

$$T_{\rm d}I_{\rm d}\frac{\partial E}{\partial t}+(I_{\rm em}+I_{\rm d})(E_{\rm ph}+E)+\frac{k_{\rm B}T}{e}\frac{\partial I_{\rm em}}{\partial x}=E_{\rm ph}I_{\rm d}, \tag{4}$$

where $I_{\rm d}=\beta/s$ is the dark irradiance, $T_{\rm d}=(\varepsilon_0\varepsilon_{\rm r}/e\mu)\times[\gamma_{\rm a}N_{\rm a}/\beta N_{\rm d}-N_{\rm a})]$ is the dielectric relaxation time without an illumination field, and $E_{\rm ph}=\beta_{\rm ph}\gamma N_{\rm a}/e\mu s$ is the PV field. By employing the initial condition $E(t=0)=0$ and slowly varying the amplitude approximation of the light intensity $I_{\rm em}$, the space-charge field E in Eq.(4) can be expressed in the following form

$$E=\left(\frac{E_{\rm ph}I_{\rm em}}{I_{\rm em}+I_{\rm d}}-\frac{k_{\rm B}T}{e}\frac{1}{I_{\rm em}+I_{\rm d}}\frac{\partial I_{\rm em}}{\partial x}\right)\times\left[\exp\left(-\frac{I_{\rm em}+I_{\rm d}}{T_{\rm d}I_{\rm d}}t\right)-1\right]. \tag{5}$$

In the PR medium, solitons can be generated when the natural light diffraction is exactly compensated for by the focusing effect. The stationary (no diffraction) solution can be written as

$$A(x,z)=\sqrt{rI_{\rm d}}\cdot u(x)\exp({\rm i}\Gamma z), \tag{6}$$

where Γ is the soliton propagate constant, and $r=I_{\max}/I_{\rm d}$ is the ratio of soliton peak intensity to dark irradiance; $u(x)$ is the normalized soliton profile which depends only on x. Substituting space-charge field E into the wave propagation equation with refractive index variation $\Delta n=-n_0^3r_{\rm eff}E/2$, the soliton propagation equation becomes

$$u''(x)=2kd^2\Gamma u(x)\pm\frac{r|u(X)|^2}{1+r|u(X)|^2}\times\left[-1+\exp\left(-\frac{1+r|u(X)|^2}{T_{\rm d}}t\right)\right]u(X), \tag{7}$$

where $r_{\rm eff}$ is the effective electro-optic coefficient of crystal, $X = x/d$ is the dimensionless variable with $d = (|k^2 n_0^2 r_{\rm eff} E_{\rm ph}|)^{-0.5}$. The sign in the second part of Eq.(7) is identical to $-r_{\rm eff}\beta_{\rm ph}$. Thus, we express dark (bright) solitons by using the plus (minus) sign.

The dark soliton's temporal behaviour can be obtained by numerical integration of Eq.(7). It reveals that changing r gives rise to two different time evolution regimes of intensity FWHM. Figure 1 depicts the FWHM of dark solitons as a function of $\tau = t/T_{\rm d}$ for various values of $r < 1$, where the solid curve represents the $r = 0.1$ case, the dotted curve represents the $r = 0.5$ case, and the dashed line represents the $r = 1$ case. From Fig.1, it can be seen that the FWHM of solitons decreases monotonically with τ and finally approaches a constant. The width of the steady soliton decreases with increasing r.

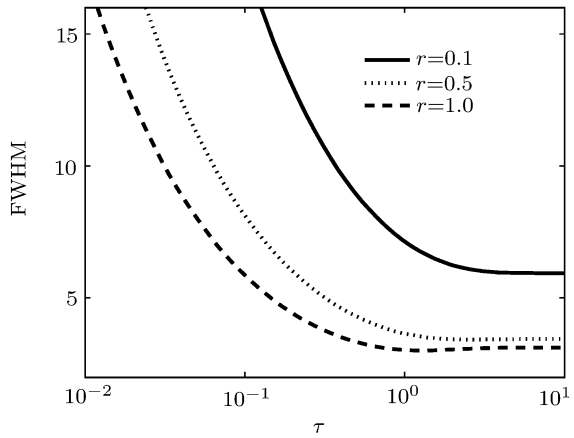


Fig.1. The FWHM of solitons versus time for $r < 1$. From the top line to the bottom one, r is equal to 0.1, 0.5 and 1, respectively.

Figure 2 exhibits the FWHM of dark solitons as a function of τ for r equal to 10, 50 and 100. From Fig.2, it is seen that the FWHM of the solitons first decreases with τ to a minimum, and then increases to a steady-state regime. The width of steady solitons increases with increasing r. Note that the time needed to reach the minimum transient intensity FWHM of the quasi-steady-state soliton is defined as its formation time.[13] Figure 2 shows that the formation time of quasi-steady-solitons decreases with increasing r.

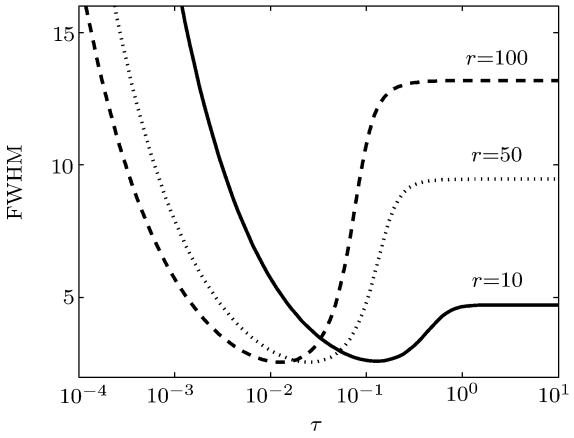


Fig.2. The FWHM of solitons versus time for $r > 1$. From the top curve to the bottom one, r equals to 100, 50 and 10, respectively.

By applying boundary conditions of dark solitons $u(\infty) = 1$ and $u''(\infty) = 0$ in Eq.(7), the propagation constant can be obtained

$$\Gamma = \frac{r}{2kd^2(1+r)}\left[1 - \exp\left(-\frac{1+r}{T_{\rm d}}t\right)\right]. \quad (8)$$

Then integrating Eq.(7) yields

$$\begin{aligned} u'^2(X) = {} & (2kd^2\Gamma - 1)[u^2(X) - 1] + \frac{1}{r}\ln\frac{1 + r|u(X)|^2}{1+r} \\ & - \frac{T_{\rm d}}{rt}\left\{\exp\left[-\frac{t}{T_{\rm d}}(1 + r|u(X)|^2)\right] - \exp\left[-\frac{t}{T_{\rm d}}(1+r)\right]\right\} \\ & - \frac{1}{r}\left\{E_{\rm i}\left[-\frac{t}{T_{\rm d}}(1 + r|u(X)|^2)\right] - E_{\rm i}\left[-\frac{t}{T_{\rm d}}(1+r)\right]\right\}, \end{aligned} \quad (9)$$

where

$$E_{\rm i}(\theta) = -\int_{-\theta}^{\infty}\frac{\exp(-y)}{y}{\rm d}y.$$

For a given time, one can obtain the soliton profile $u(X)$ by solving Eq.(9). Figure 3 shows the soliton intensity profile $u^2(X)$ at different special time for $r = 10$. In the early evolution time $\tau = 0.001$, a wide soliton forms inside the crystal because the spatial charge field is low and the diffraction effect

dominates. With increasing time, the spatial charge field builds up with the photo-induced refractive index changing dramatically. As a result, the width of the soliton narrows. When $\tau = 0.12$, the width of the solitons reaches its minimum. As time further evolves, the width of the solitons becomes wider than that at $\tau = 0.12$. After $\tau = 1$, the spatial charge field reaches the steady state and the width of the soliton remains constant. These results agree well with those in Fig.2 for the case of $r = 10$.

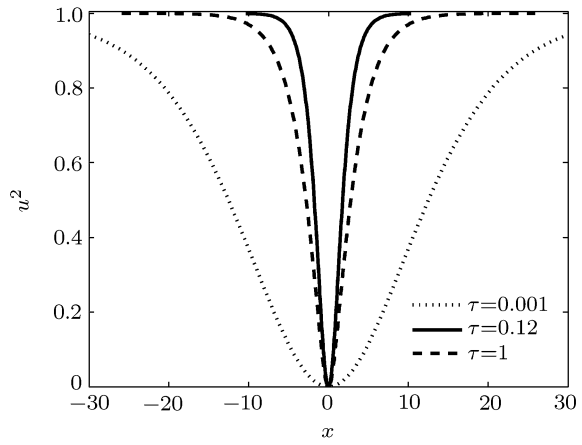


Fig.3. The intensity profiles of dark solitons for $r = 10$ at $\tau = 0.001$ (dotted line), $\tau = 0.12$ (solid line), and $\tau = 1$ (dashed line).

In iron-doped $LiNbO_3$ crystals light tends to decrease the refractive index induced by PR effect. We noted that the sign of Δn is identical to that of $r_{\rm eff}\beta_{\rm ph}$, whereas the sign of electrooptic coefficient $r_{\rm eff}$ is opposite to that of $\beta_{\rm ph}$. This character indicates that the dark solitons can be observed in $LiNbO_3$ crystal. In this theory we assume that the spatial solitons are formed at all times during the spacecharge field buildup. Achieving this condition, we need to dynamically adjust the width of dark ditch at the entrance face of the crystal to the width of the ditch at the exit face. Although this is not strictly fulfilled in the experiment described below, the results qualitatively agree with the theory. A similar method employed in strontium barium niobate (SBN) crystal has been successful.[16]

3. Experiment

3.1. Experimental setup

The experimental apparatus is depicted schematically in Fig.4. We use $LiNbO_3$:Fe crystal with a c-axis along the x direction, and launch an e-polarized beam ($\lambda = 488$ nm) to exploit the large electro-optic coefficient r_{33}. To observe dark planar solitons, we expand the laser beam by the beam expander EL, and then insert a glass microscope cover slide G in a half beam. Tilting G, when the phase is equal to $\phi = (2n+1)\pi$, we obtain a dark notch with some higher-order diffraction fringes. In order to eliminate the higher order fringes, we use a 4F system composed of G, lens L1, slit and lens L2. The spatial filtered beam is focused by the cylindrical lens CL to the entrance face of the crystal. After the crystal, we set a polarizer P2 to moderate the beam intensity which is imaged into a microscope objective L3 and a CCD camera. Varying the distance between the CCD and crystal, we can obtain pictures on the entrance and exit faces. A computer is connected to the CCD camera to acquire images and extract the relevant characters. The FWHM of the dark notch is evaluated to within ± 0.5 μm.

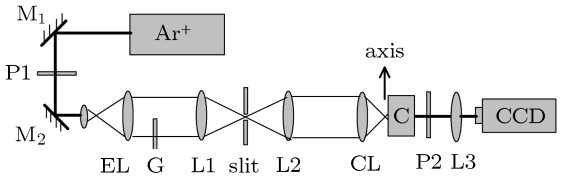


Fig.4. The experimental setup. M_1, M_2, mirror; P1, P2, polarizer; EL, beam expander; G, glass slide; L1-L2, spherical lenses; slit; CL, cylinder lens; C, crystal; L3, microscope objective; CCD, CCD camera.

3.2. The dark solitons experiment

First, we let a 10 μW laser beam having an 18 μm notch focus onto the entrance face of a 8.6 cm long crystal, as shown in Fig.5(a). At $t = 0$, the dark notch at the crystal exit face diffracts to 63 μm, as depicted in Fig.5(b) . Under beam illumination, the dark ditch becomes narrow for stronger PR effect. For about an hour, the notch reaches steady state with a width of 18 μm in Fig.5(c). Horizontal intensity profiles at the crystal entrance face and exit face with different time of illumination are below the pictures. These results indicate that dark PV solitons have formed.

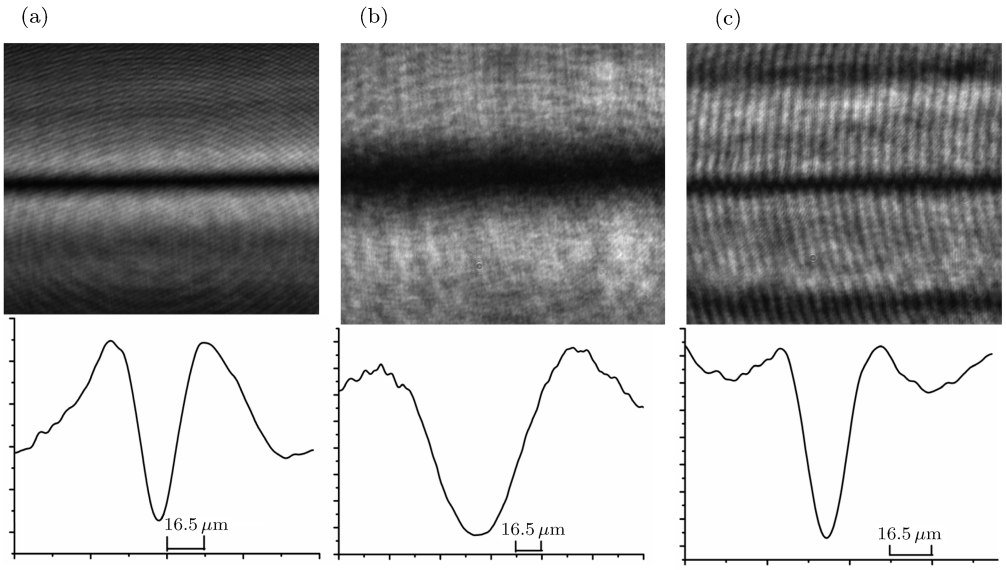


Fig.5. Pictures of dark solitons and the horizontal intensity profiles. (a) The input beam, (b) the diffractive beam at the exit face, (c) dark solitons at $t = 60$ min.

We then let the laser beam be equal to 10, 20 and 50 μW, respectively, and use a CCD camera to acquire the images of the output beam at regular intervals. Fitting the size of the dark notch at different time, we obtain the evolution curve of the dark solitons, as displayed in Fig.6, where circles represent the case of 10 μW, triangles represent the case of 20 μW, and squares represent the case of 50 μW. In Fig.6, the width of solitons decreases monotonically with time and finally reaches a constant value. The widths of steady solitons are 21, 18 and 13 μm from the top curve to the bottom one. These experimental results agree well with the theory analysis in the range of $r < 1$.

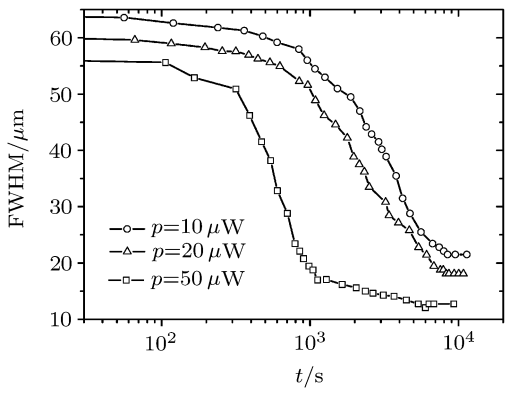


Fig.6. Dark-notch intensity FWHM evolution for beam power of 10 μW, 20 μW and 30 μW ,respectively, from the top line to the bottom one.

In Fig.7, curves are measured with a 2mm-long crystal, and the power of the laser beam is equal to 1 mW, 500 μW and 300 μW. All curves begin with an initial FWHM of 15 μm. By changing the laser beam power, the dark notch undergoes a self focusing effect followed by some widening. Figure 7 shows that the width of the solitons attains the same minimum at different powers, but the minimum occurs earlier in time for high power, as predicted in Fig.2. For a fixed beam intensity, changing the size of the dark notch at the crystal entrance face from 20 μm to 10 μm, we still gain the same minimum approximately 5 μm. These features demonstrate that the quasi-steady-state solitons have formed in the PV material.

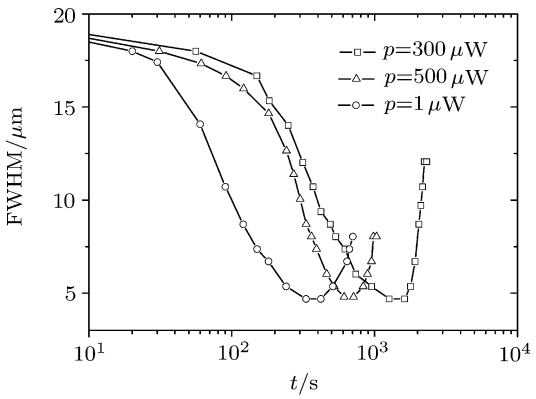


Fig.7. Dark-notch intensity FWHM evolution for various beam powers. Squares, 300 μW; triangles, 500 μW; circles, 1 mW.

In addition, we observe that the formation time of quasi-steady-state solitons is inversely proportional to the intensity of the laser beam, as depicted in Fig.8. In these experiments, quasi-steady-state solitons are obtained only because of modulation instability. By comparing the experimental curves with the results of the numerical integration in Fig.2, the qualitative agreement is obvious.

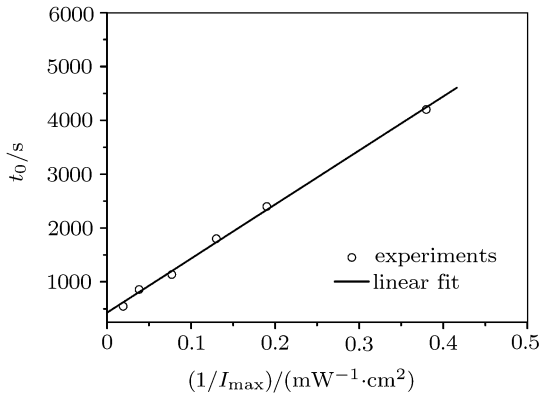


Fig.8. Measurement of quasi-steady-state dark PV soliton formation time t_0 as a function of $1/I_{\max}$.

3.3. The experimental analysis

In our experiments, r equals the ratio of soliton peak intensity to dark irradiance, which is the key parameter in the evolution of dark solitons. The typical value of dark irradiance in $LiNbO_3$:Fe crystal is 1 mW/cm^2. We calculate beam intensity by the formula of $I = P/S$, where P is optical power and S is the area of the beam on the crystal. In Fig.6, the beam intensities are all below 1 mW/cm^2, which meets the case of $r < 1$. In this situation, we find that the FWHM of the dark notch decreases monotonically with time, and the width of the steady solitons decreases with increasing r. These experimental results are in concordance with the theory for $r < 1$. We then enhanced the beam intensity to about 9 mW/cm^2, 15 mW/cm^2 and 30 mW/cm^2 in Fig.7, which meet the case of $r > 1$. Under these conditions, we have obtained quasi-steady-state solitons only with formation time inversely proportional to the intensity. The evolution of dark solitons agrees with the theory in the quasi-steady-state regime but not the steady-state regime because of beam breakup. In dark PV solitons experiment, modulation instability is the main factor inhibiting the formation of steady solitons, and it is enhanced exponentially with increasing beam intensity and crystal length.[17,18] In order to reduce the modulation instability, we have chosen a shorter crystal at high intensities, but it cannot be eliminated. Ignoring this limitation, the quantitative coincidence is excellent.

4. Conclusions

In conclusion, we have presented detailed results of the experimental observation of the dark PV solitons in iron-doped $LiNbO_3$ crystal, and compared these results with those based on the time-dependent band-transport model. We proved theoretically that dark PV solitons can exist in both the quasi-steady-state and steady-state regimes. For $r < 1$, the FWHM of the dark PV solitons decreases monotonically to a constant value, whereas for $r > 1$, the FWHM of the solitons first decreases to a minimum, and then increases to a constant value. Moreover, the FWHM of the steady solitons decreases with increasing r for $r < 1$, and increases with increasing r for $r > 1$. We did experiments at both low and high beam powers, and obtained the temporal behaviours of the solitons. The experimental results demonstrated that steady solitons can be observed at low optical intensities, while the quasi-steady-state solitons exist only at higher beam power with the FWHM being 5 μm wide. These experimental results agree well with our theory, and more importantly, this is the first time one has observed the quasi-steady solitons in $LiNbO_3$:Fe crystal.

References

[1] Shi T T and Chi S 1990 *Opt. Lett.* **15** 1123

[2] Segev M, Crosignani B, Yariv A and Fisher B 1992 *Phys. Rev. Lett.* **68** 923

[3] He G G, Wang X S and She W L 2002 *Acta Phys. Sin.* **51** 2270 (in Chinese)

[4] Christodoulides D N and Carvalho M I 1995 *J. Opt. Soc. Am.* B **12** 1628

[5] Taya M, Bashaw M, Fejer M M, Segev M and Valley G C 1995 *Phys. Rev.* A **52** 3095

[6] Li J P, Lu K Q, Zhao W, Yang Y L, Zhu X P, and Guo X H 2005 *Chin. Phys. Lett.* **22** 1423

[7] Liu J S, Zhang H L, Zhang G Y and Wang C 2006 *Chin. Phys.* **15** 394

[8] Chen Z, Mitchell M, Shih M, Segev M, Garret M H and Valley G C 1996 *Opt. Lett.* **21** 629

[9] Segev M, Shih M and Valley G C 1996 *J. Opt. Soc. Am.* B **13** 706

[10] Chauvet M, Chauvin S and Maillotte H 2001 *Opt. Lett.* **26** 1344

[11] She W L, Lee K K and Lee W K 1999 *Phys. Rev. Lett.* **83** 3182

[12] Morin M, Duree G, Salamo G and Segev M 1995 *Opt. Lett.* **20** 2066

[13] Fressengeas N, Maufoy J and Kugel G 1996 *Phys. Rev.* E **54** 6866.

[14] Lu K Q, Zhao W, Zhang L, Li K H, Zhang Y Q, Liu X M, Zhang Y P and Xu J J 2008 *Opt. Commun.* **281** 2913

[15] Chauvet M 2003 *J. Opt. Soc. Am.* B **20** 2515

[16] Wesner M, Herden C, Pankrath R, Kip D and Moretti P 2001 *Phys. Rev.* E **64** 036613

[17] Zhu N, Guo R, Liu S M, Liu Z H and Song T 2006 *J. Opt.* A: *Pure Appl. Opt.* **8** 149

[18] Lu K Q, Zhao W, Yang Y L, Zhu X P, Li J P and Zhang Y P 2004 *Chin. Phys.* **13** 2077